

Highly Sensitive Electrochemical Detection of Paraquat in Environmental Water Samples Using a Vertically Ordered Mesoporous Silica Film and a Nanocarbon Composite

Weiran Zheng ^{1,*}, Ruobing Su ², Guoguang Yu ¹, Lin Liu ¹ and Fei Yan ^{2,*}

¹ Institute of Agro-product Safety and Nutrition, Zhejiang Academy of Agricultural Sciences, Hangzhou 310021, China

² Key Laboratory of Surface & Interface Science of Polymer Materials of Zhejiang Province, Department of Chemistry, Zhejiang Sci-Tech University, Hangzhou 310018, China

* Correspondence: rancki@163.com (W.Z.); yanfei@zstu.edu.cn (F.Y.)

S1 CV curves of bare GCE and VMSF/3DG-CNT/GCE in deoxygenated PBS

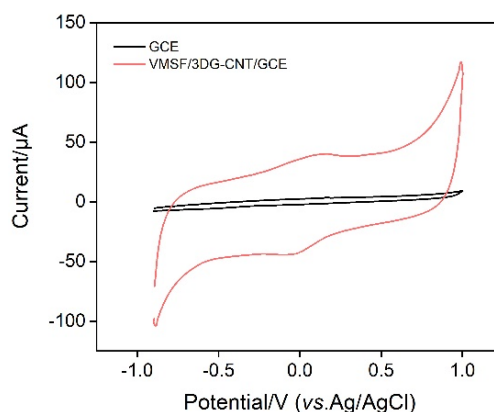


Figure S1. CV curves of bare GCE (black) and VMSF/3DG-CNT/GCE (red) in deoxygenated PBS (0.1 M, pH = 6).

S2 Optimization of experimental conditions

S2.1 Electrodeposition time of 3DG-CNT

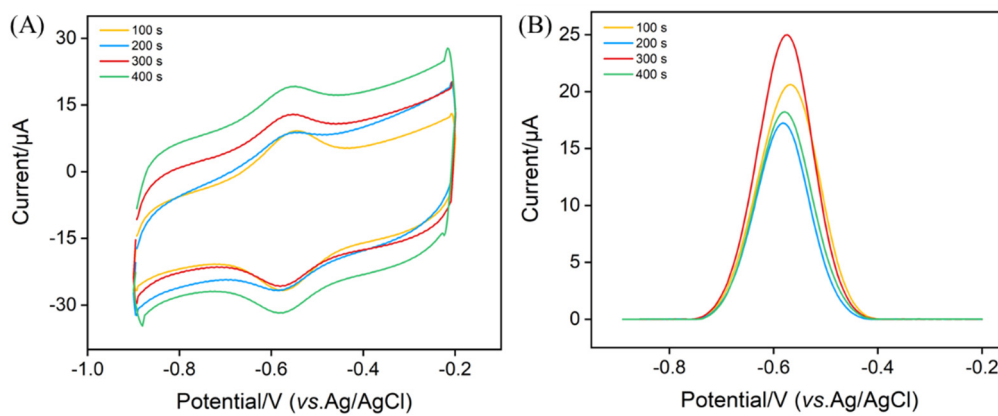


Figure S2.1 (A) CVs and (B) DPVs obtained at the 3DG-CNT/GCE electrodeposited under the potential of -1.2 V for various times in 0.1 M PBS ($\text{pH} = 6$) containing 3.5 μM PQ.

S2.2 Growth time of VMSF

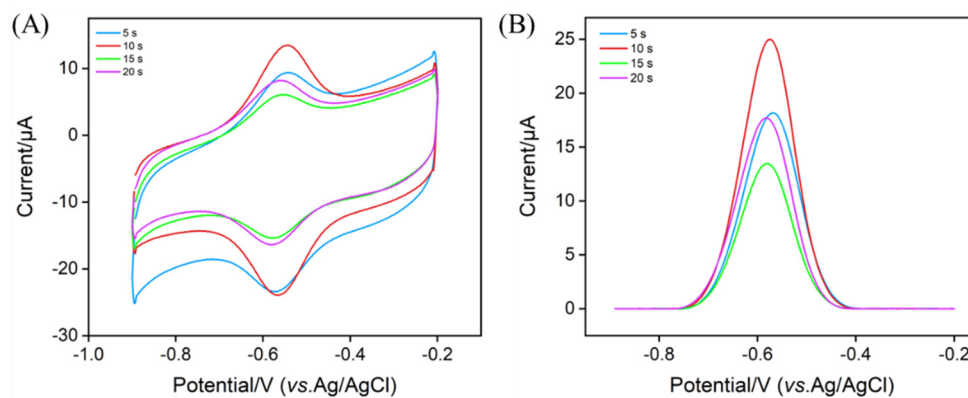


Figure S2.2 (A) CVs and (B) DPVs obtained at the VMSF/3DG-CNT/GCE under different growth times of VMSF in 0.1 M PBS ($\text{pH} = 6$) containing 3.5 μM PQ.

S2.3 pH of supporting electrolyte

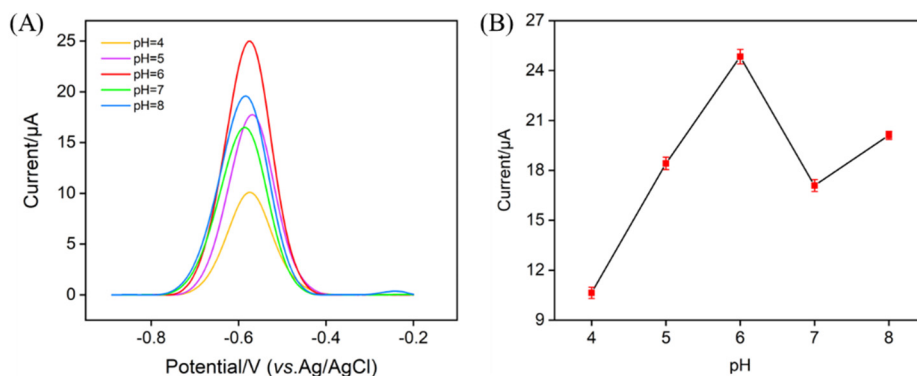


Figure S2.3 (A) DPV curves obtained at the VMSEF/3DG-CNT/GCE in 0.1 M PBS containing 3.5 μ M PQ at various pH values. (B) Effect of the pH value of PBS on the detection of PQ. The error bars represent the SD of three measurements.

S2.4 Concentration of supporting electrolyte

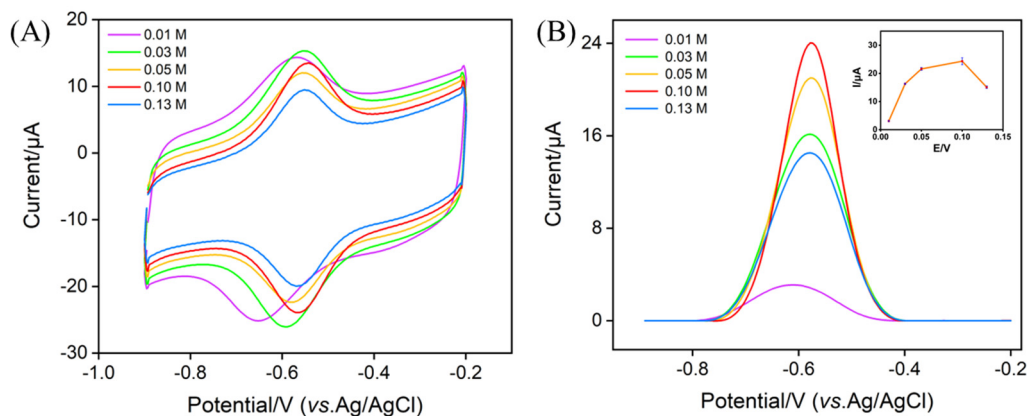


Figure S2.4 (A) CVs and (B) DPVs obtained at the VMSEF/3DG-CNT/GCE in response to 3.5 μ M PQ at various concentrations of PBS (pH = 6). Inset is the concentration of PBS on the detection of PQ. The error bars represent the SD of three measurements.



S2.5 Preconcentration time

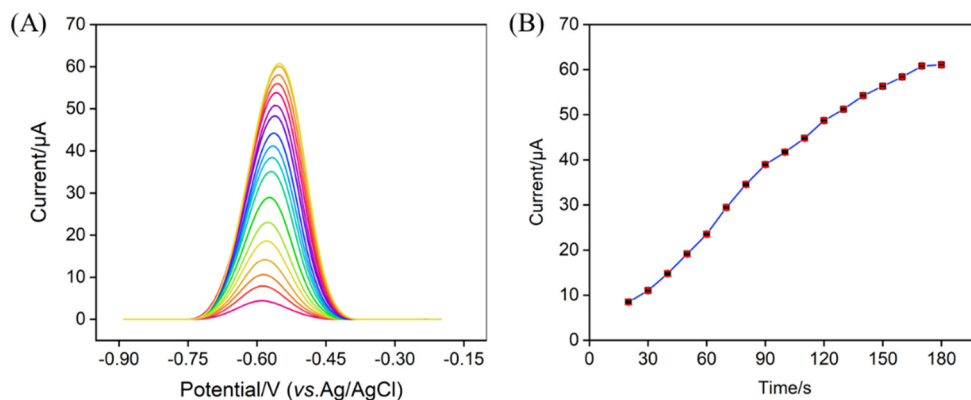


Figure S2.5 (A) DPVs obtained at the VMSF/3DG-CNT/GCE in 0.1 M PBS (pH = 6) containing 10 μM PQ at various mechanical stirring time. (B) The dependence of anodic peak current on the preconcentration time.

S3 Anti-interference ability, repeatability and stability of VMSF/3DG-CNT/GCE

S3.1 Anti-interference ability of VMSF/3DG-CNT/GCE

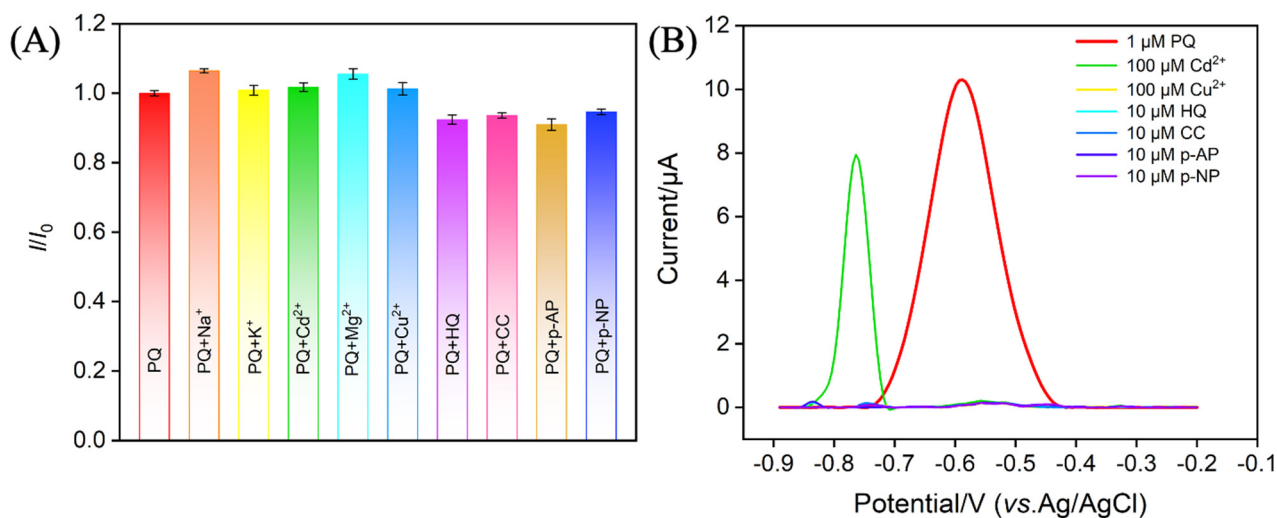


Figure S3.1 (A) The current ratio (I/I_0) obtained from VMSF/3DG-CNT/GCE for detection of PQ (1 μM) in the absence (I_0) and presence (I) of 100-fold (Na^+ , K^+ , Cd^{2+} , Mg^{2+} , and Cu^{2+}) or 10-fold of HQ, CC, p-AP and p-NP. The error bars represent the SD of three measurements. **(B)** DPV curves of the VMSF/3DG-CNT/GCE for detection of PQ, Cd^{2+} , Cu^{2+} , HQ, CC, p-AP or p-NP.

S3.2 Repeatability of VMSF/3DG-CNT/GCE

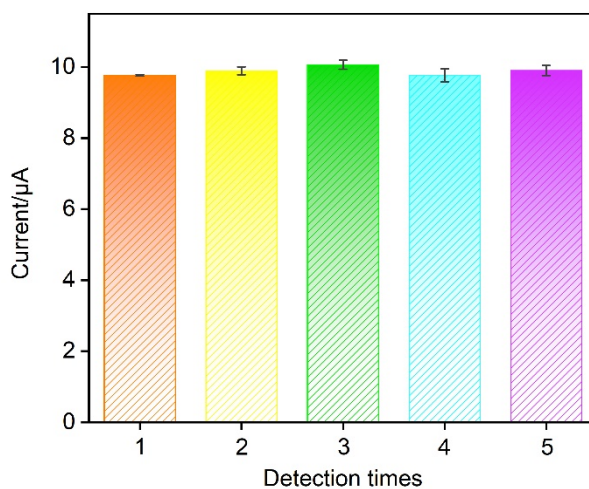


Figure S3.2 Repeatability of VMSF/3DG-CNT/GCE in the presence of 1 μM PQ.



S3.3 Stability of VMSF/3DG-CNT/GCE

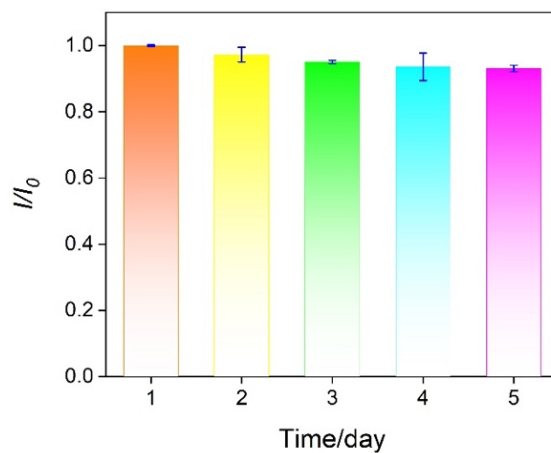


Figure S3.3 Stability of the VMSF/3DG-CNT/GCE. I and I_0 denote the anodic peak current measured at various days and initial measured value, respectively.